The protein phosphatase 2A functions in the spindle position checkpoint by regulating the checkpoint kinase Kin4

Citation: Chan, L. Y., and A. Amon. "The Protein Phosphatase 2A Functions in the Spindle Position Checkpoint by Regulating the Checkpoint Kinase Kin4." Genes & Development 23.14 (2009): 1639–1649. CrossRef. Web.

As Published: http://dx.doi.org/10.1101/gad.1804609

Publisher: Cold Spring Harbor Laboratory Press

Persistent URL: http://hdl.handle.net/1721.1/77594

Version: Author's final manuscript: final author's manuscript post peer review, without publisher's formatting or copy editing

The Protein Phosphatase 2A functions in the spindle position checkpoint by regulating the checkpoint kinase Kin4.

Leon Y. Chan and Angelika Amon[1]

David H. Koch Institute for Integrative Cancer Research and
Howard Hughes Medical Institute
Massachusetts Institute of Technology, E17-233
40 Ames Street
Cambridge MA 02139
USA

[1] To whom correspondence should be addressed.
e-mail: angelika@mit.edu

Abstract

In budding yeast, a surveillance mechanism known as the spindle position checkpoint (SPOC) ensures accurate genome partitioning. In the event of spindle mis-position the checkpoint delays exit from mitosis by restraining the activity of the mitotic exit network (MEN). To date, the only component of the checkpoint to be identified is the protein kinase Kin4. Furthermore, how the kinase is regulated by spindle position is not known. Here, we identify the protein phosphatase PP2A in complex with the regulatory subunit, Rts1, as a component of the SPOC. Loss of PP2A-Rts1 function abrogates the spindle position checkpoint but not other mitotic checkpoints. We further show that the protein phosphatase functions upstream of Kin4, regulating the kinase's phosphorylation and localization during an unperturbed cell cycle and during spindle position checkpoint activation thus defining the phosphatase as a key regulator of SPOC function.

Introduction

Many cell divisions are polarized, with intrinsic and/or extrinsic cues dictating the directionality of cell division. To ensure that the genetic material is segregated accurately during polarized division, the mitotic spindle must be positioned according to these polarization cues. There is mounting evidence to suggest that this process of spindle positioning is coupled to the cell cycle. In cultured rat kidney cells, a delay in anaphase onset occurs when the metaphase spindle is mis-positioned (O'Connell and Wang 2000). In Drosophila male germline stem cells, cell cycle progression also appears delayed when the spindle is mis-positioned (Cheng, Turkel et al. 2008). Such coupling is suggestive of a feedback mechanism that delays the cell cycle in response to defects in spindle position.

A surveillance mechanism that delays the cell cycle in response to defects in spindle position has been described in the budding yeast, *Saccharomyces cerevisiae*, and is termed the spindle position checkpoint (SPOC) (Yeh, Skibbens et al. 1995). Each cell division of budding yeast is asymmetric and thus inherently polarized. Budding yeast cells divide by forming a bud and hence determine the site of cytokinesis during entry into the cell cycle long before the mitotic spindle is formed. This manner of dividing requires the active positioning of the mitotic spindle along this predetermined division axis, which is known in yeast as the mother-bud axis. The spindle position checkpoint ensures proper spindle position and thus chromosome segregation by delaying exit from mitosis, specifically anaphase spindle disassembly and cytokinesis, until the spindle is correctly positioned along the mother-bud axis (Yeh, Skibbens et al. 1995). The function of the SPOC is most apparent in cells deficient in cytoplasmic microtubule dynamics, guidance and capture. Such cells fail to position the mitotic spindle along the division axis resulting in anaphase spindle elongation in the mother cell(Yeh, Skibbens et al. 1995). Failure of this checkpoint results in the formation of anucleated and multi-nucleated cells.

The spindle position checkpoint delays exit from mitosis by inhibiting the mitotic exit network (MEN). The MEN is a signal transduction pathway whose activity is controlled by the small GTPase, Tem1(Shirayama, Matsui et al. 1994). Tem1 regulates a kinase

cascade, whose activation ultimately leads to a sustained release of the phosphatase Cdc14 from its nucleolar inhibitor Cfi1/Net1(Shirayama, Matsui et al. 1994; Shou, Seol et al. 1999; Visintin, Hwang et al. 1999; Bardin, Visintin et al. 2000; Lee, Frenz et al. 2001; Luca, Mody et al. 2001; Mah, Jang et al. 2001). Once released, Cdc14 dephosphorylates key substrates to bring about exit from mitosis(Visintin, Craig et al. 1998; Zachariae, Schwab et al. 1998; Jaspersen, Charles et al. 1999; Bardin, Visintin et al. 2000).

Several proteins have been identified that regulate Tem1 during the cell cycle and in response to spindle position defects. Tem1 is controlled positively by the bud cortex restricted protein, Lte1 (which resembles a guanine nucleotide exchange factor; GEF) and negatively by the two-component GTPase activating protein (GAP), Bub2-Bfa1(Shirayama, Matsui et al. 1994; Lee, Hwang et al. 1999; Li 1999; Bardin, Visintin et al. 2000; Bloecher, Venturi et al. 2000; Pereira, Hofken et al. 2000; Geymonat, Spanos et al. 2002). In the absence of *LTE1*, cells fail to activate the MEN and do not exit from mitosis at low temperatures (Shirayama, Matsui et al. 1994). The absence of the GAP leads to inappropriate MEN activation and mitotic exit in cells arrested in mitosis due to activation of the spindle assembly checkpoint (SAC) or the SPOC (Hoyt, Totis et al. 1991; Fesquet, Fitzpatrick et al. 1999; Bardin, Visintin et al. 2000; Bloecher, Venturi et al. 2000; Pereira, Hofken et al. 2000). A single spindle position checkpoint specific regulator of the MEN has also been identified. The protein kinase Kin4 is only required for MEN inhibition in response to spindle position defects(D'Aquino, Monje-Casas et al. 2005; Pereira and Schiebel 2005). Kin4 localizes to the mother cell cortex throughout most of the cell cycle. During anaphase the protein kinase also localizes to the spindle pole body (SPB) that remains in the mother cell (D'Aquino, Monje-Casas et al. 2005; Pereira and Schiebel 2005). In cells with mis-positioned spindles, Kin4 associates with both SPBs where it phosphorylates Bfa1(Pereira and Schiebel 2005; Maekawa, Priest et al. 2007). This phosphorylation protects the GAP from inhibitory phosphorylation by the Polo kinase, Cdc5, effectively locking Bub2-Bfa1 in an active state thus inhibiting the MEN (Hu, Wang et al. 2001; Geymonat, Spanos et al. 2003; Maekawa, Priest et al.

2007). How Kin4 itself is controlled during the cell cycle or in response to spindle position defects is not understood.

Here, we identify the protein phosphatase PP2A-Rts1 as a regulator of Kin4 function. PP2A-Rts1 is required for the dephosphorylation of Kin4 during cell cycle entry and to maintain Kin4 in the dephosphorylated state during S-phase and mitosis. Furthermore the phosphatase controls the association of Kin4 with SPBs both during the cell cycle and in response to spindle position defects. The importance of this control is underlined by the finding that PP2A-Rts1 is essential for spindle position checkpoint function but not for other mitotic checkpoints. We propose that PP2A-Rts1 is a SPOC component that facilitates Kin4 localization thereby restraining MEN activity.

Results

PP2A-Rts1 regulates Kin4 phosphorylation.

Kin4 is essential for spindle position checkpoint function. To determine how the protein kinase is controlled, we focused on its previously observed cell cycle regulated phosphorylation. Phosphorylated Kin4 can be detected as slower migrating species by SDS-PAGE(D'Aquino, Monje-Casas et al. 2005). Kin4 is phosphorylated in G1, but upon release from a pheromone induced G1-arrest, Kin4 phosphorylation is rapidly lost. The protein remains in a hypophosphorylated state throughout S phase and mitosis, but is rapidly rephosphorylated during exit from mitosis (Figure 1A and (D'Aquino, Monje-Casas et al. 2005)).

Kin4 is in the dephosphorylated state during the stages of the cell cycle when Kin4 activity is needed to inhibit the MEN in response to potential spindle position defects. This correlation prompted us to investigate the significance of Kin4 phosphorylation by identifying phosphatases responsible for dephosphorylating Kin4. We screened mutants defective in known cell cycle associated phosphatases for effects on Kin4 phosphorylation. Kin4 phosphorylation was examined in cells harboring temperature sensitive alleles of *CDC14 (cdc14-3), SIT4 (sit4-102*,(Wang, Wang et al. 2003)), Protein Phosphatase 1 (PP1; *glc7-12*), and a combination of alleles that renders the Protein

Phosphatase 2A (PP2A) temperature sensitive (*pph3Δ, pph21Δ, pph22-12*; henceforth temperature sensitive PP2A, (Evans and Stark 1997)). We grew the cells to mid exponential phase at permissive temperature (23°C) and followed Kin4 phosphorylation upon shift to the restrictive temperature (37°C). Temperature shift led to a transient accumulation of hyperphosphorylated Kin4 even in wild-type cells, for unknown reasons, which was particularly evident when the ratio of phosphorylated to unphosphorylated Kin4 was determined (Figure 1B, C). After the transient accumulation of hyperphosphorylated Kin4, however, both hyper and hypophosphorylated Kin4 were detected in wild-type and most phosphatase mutants. The *sit4-102* mutant displayed hyperphosphorylation after temperature shift, which was progressively lost during incubation at 37°C (Figure 1B, C). Temperature sensitive PP2A mutants showed a persistence of hyper-phosphorylated Kin4 (Figure 1B-C). Though other phosphatases, possibly Sit4, contribute to Kin4 dephosphorylation (see also Figure 3B), we conclude that PP2A is primarily required for Kin4 de-phosphorylation.

Budding yeast PP2A is a heterotrimeric enzyme composed of a single scaffolding subunit, Tpd3, a catalytic subunit, Pph21 or Pph22 and a regulatory subunit, Cdc55 (B type-PP2A) or Rts1 (B' type-PP2A) (reviewed in (Jiang 2006)). To determine which regulatory subunit is required for Kin4 dephosphorylation, we examined the phosphorylation status of Kin4 in the *cdc55*Δ and *rts1*Δ mutants. In *cdc55*Δ cells, Kin4 phosphorylation status resembled that of wild-type. In contrast, in the *rts1*Δ strain, Kin4 phosphorylation resembled that of the PP2A mutant (Figure 1B, C). We conclude that PP2A-Rts1 is primarily responsible for Kin4 dephosphorylation.

PP2A-Rts1 is a component of the spindle position checkpoint.

If dephosphorylation of Kin4 is important for its checkpoint function, mutants in which Kin4 dephosphorylation is impaired should exhibit spindle position checkpoint defects. To test this possibility, we examined how *PP2A-RTS1* mutants respond to spindle mis-position. Cells lacking cytoplasmic dynein (*dyn1*Δ) exhibit spindle position defects particularly at low temperature (14°C)(Li, Yeh et al. 1993). As a result, chromosome segregation frequently occurs within the mother cell. This in turn leads to activation of

the SPOC, which causes inhibition of the MEN and cell cycle arrest in late anaphase ("arrested" morphology; Figure 2A). *dyn1*Δ cells with an impaired SPOC fail to delay mitotic exit resulting in anucleated and multinucleated cells ("bypassed" morphology; Figure 2A).

After growth at 14°C for 24 hours, 27% of *dyn1*Δ mutants exhibit the "arrested" morphology and only 10% the "bypassed" morphology (Figure 2B), indicating that the SPOC is functional and that the MEN is inhibited. When the SPOC is inactivated by deletion of *KIN4,* 35% of *dyn1*Δ *kin4*Δ double mutant cells exhibit the "bypassed" morphology. Deletion of *RTS1* in the *dyn1Δ* mutant also lead to inactivation of the SPOC with 42% of cells showing the "bypassed" morphology (Figure 2B). Importantly, the *rts1*Δ single mutant did not exhibit spindle position defects indicating that PP2A-Rts1 likely does not play a role in the actual positioning of the spindle. The spindle position checkpoint defect was specific to PP2A-B' as the *cdc55Δ dyn1*Δ mutant displayed no SPOC defect (Figure 2B). We observed a defect in SPOC function in *dyn1*Δ *pph21*Δ *pph22-12 pph3*Δ quadruple mutants although this defect was not as pronounced as in the *dyn1Δ rts1Δ* mutant possibly due to the proliferation defect of the quadruple mutant (Figure 2B). Lastly, we found that deletion of *KIN4* did not enhance the SPOC defect of *dyn1*Δ *rts1*Δ mutants. Taken together, these data indicate that PP2A-Rts1 is a component of the SPOC that likely functions in the same pathway as *KIN4*.

PP2A-Rts1 functions in the SPOC by controlling Kin4 localization to spindle pole bodies.

Having established that PP2A-Rts1 is required for SPOC function, we wished to determine whether PP2A-Rts1 acts through Kin4. To this end we examined the effects of deleting *RTS1* on the phenotype associated with *KIN4* overexpression. Overexpression of *KIN4* from the *GAL1-10* promoter terminally arrests cells in anaphase (D'Aquino, Monje-Casas et al. 2005). Deletion of *RTS1* suppressed the lethality caused by *GAL-KIN4* (Figure 3A) indicating that overexpressed Kin4 requires PP2A-Rts1 function to exert its inhibitory effects on mitotic exit. Importantly, deletion of *RTS1* did not suppress the lethal anaphase arrest induced by *GAL-BFA1* (Lee, Hwang et al. 1999; Li 1999)

suggesting that *rts1*Δ is not a general suppressor of anaphase arrest but instead shows specificity towards *KIN4*. The rescue of the *GAL-KIN4* lethality by the deletion of *RTS1* was not as complete as that brought about by the deletion of *BUB2*, a gene known to function downstream of *KIN4*, suggesting that the mechanisms of suppression may not be the same ((D'Aquino, Monje-Casas et al. 2005); Figure 3A).

To determine the relationship between PP2A-Rts1 and Kin4 we examined the effects of deleting *RTS1* on Kin4 phosphorylation, activity and localization. We found that Kin4 is hyper-phosphorylated throughout the cell cycle in the *rts1*Δ mutant (Figure 3B). While we observed a consistent 10 to 15 minute delay in cell cycle progression prior to metaphase spindle assembly, inactivation of *RTS1* did not affect the phosphorylation state of the Bub2-Bfa1 complex, nor the MEN GTPase Tem1, nor the Tem1 activator Lte1, as judged by changes in electrophoretic mobility (Figure 3C – F). These findings suggest that not all SPOC components and its targets are substrates of PP2A-Rts1.

Next we examined whether PP2A-Rts1 affects Kin4 activity, which is essential for checkpoint function (Supplemental Figure 1A). Kin4 kinase activity was not decreased when isolated from *rts1*Δ mutant cells (Supplemental Figure 1B-C) indicating that PP2A-Rts1 does not affect Kin4's *in vitro* enzymatic activity.

An intact SPOC not only requires Kin4 kinase activity but also binding of the protein kinase to SPBs (Maekawa, Priest et al. 2007). During an unperturbed cell cycle Kin4 localizes to the mother cell cortex. During anaphase, Kin4 also associates with the SPB that remains in the mother cell (mSPB). In cells with mis-positioned anaphase spindles, Kin4 associates with both SPBs. Kin4 mutants that fail to localize to SPBs are checkpoint defective (Maekawa, Priest et al. 2007). Furthermore, ectopically targeting Kin4 to SPBs suffices to delay mitotic exit (Maekawa, Priest et al. 2007). We monitored the ability of Kin4-GFP to associate with the mSPB during anaphase and observed a strong reduction in mSPB localization in *rts1Δ* cells (Figure 4). Whereas Kin4-GFP localized to the mSPB during anaphase in 54% of wild-type cells, Kin4-GFP was found on mSPBs of only 11% of *rts1*Δ anaphase cells (Figure 4C). Furthermore, in the *rts1*Δ mutant cells that showed

Kin4 localization at the mSPB, the signal was weaker (Figure 4A). The loss of Kin4 localization to SPBs was not due to a reduction in *KIN4-GFP* expression in the *rts1*Δ mutant, as levels of Kin4-GFP in these cells are similar to that observed in wild-type cells (Figure 4B). The cortical localization and asymmetry of Kin4 was also reduced in *rts1*Δ cells which was most pronounced in small budded cells (Figure 4A, 5A, D). The basis of this loss in asymmetric localization of Kin4 is currently unclear. Localization of Bub2, Bfa1 and Tem1 was not affected by the deletion of *RTS1* (Supplemental Figures 2A-C) indicating that loss of *RTS1* function does not alter the overall structure of SPBs nor affects the localization of other SPB-associated MEN proteins. Bud restricted cortical localization of Lte1 was also not affected by deletion of *RTS1* suggesting that overall cell polarity and integrity of the bud neck is maintained in the mutant (Supplemental Figure 2D). We conclude that PP2A-Rts1 is required for Kin4 function and association of the protein with the mSPB during anaphase.

RTS1 is Required for Efficient SPB Loading of Kin4 in response to SPOC activation.

Having determined that *RTS1* was required for Kin4 localization during an unperturbed cell cycle we next investigated whether *RTS1* also affected Kin4 loading onto SPBs when the spindle is depolymerized or mis-positioned, situations where the SPOC is active and *KIN4* function would be most important. We first examined cells treated with the spindle depolymerizing drug nocodazole. Under these conditions Kin4 associates with SPBs ((Pereira and Schiebel 2005); Figure 5A, B). In contrast, Kin4 association with SPBs was significantly reduced in *rts1*Δ mutants (Figure 5A-B). In the few cells where Kin4 was detected on SPBs the signal intensity was reduced. This loss of SPB association could not be explained by changes in Kin4 expression as Kin4-GFP protein levels were similar in the two strains (Figure 5C). Similar results were obtained in *dyn1*Δ cells with mis-positioned spindles. In such cells Kin4 localizes to both SPBs ((Pereira and Schiebel 2005); Figure 5D, E). In the absence of *RTS1*, Kin4 localization to SPBs was severely impaired (Figure 5D, E).

Overexpression of *KIN4* only partially suppressed the Kin4 SPB loading defect of *rts1*Δ mutants, providing a possible explanation for why deleting *RTS1* suppressed the lethality associated with high levels of Kin4 (Figure 3A). Over-expression of *KIN4* from the *MET25* promoter, which inhibits proliferation (Figure 5F), allowed some Kin4 to associate with SPBs in *rts1*Δ mutants but the number of cells that exhibit Kin4 localization to SPBs was reduced compared to wild-type cells (Figure 5G). Thus in all situations in which Kin4 is known to load onto SPBs (correctly positioned anaphase spindles, spindle depolymerization, mis-positioned anaphase spindles and overexpressed Kin4), we observe a defect in SPB loading in the *rts1*Δ mutant.

In cells with a mis-positioned spindle and an intact SPOC, both Bub2 and Bfa1 localize to both SPBs but Tem1 fails to load onto SPBs. When *KIN4* is deleted, Tem1 loads onto SPBs and thus presumably allows for premature exit from mitosis ((D'Aquino, Monje-Casas et al. 2005); Figure 5J). Consistent with previously observed effects of loss of *KIN4* function on the localization of Tem1 complex components, both Bub2 and Bfa1 localization were unaffected by deletion of *RTS1* but Tem1 was observed to improperly load on to SPBs of cells with mis-positioned spindles (Figure 5H-J). This improper loading of Tem1 onto SPBs of cells with mis-positioned spindles in the *rts1Δ* mutant indicates that *RTS1* is required for normal *KIN4* function.

***RTS1* inhibition of the MEN is spindle position checkpoint specific.**

Our data show that PP2A-Rts1 inhibits the MEN when the SPOC is active. We next wished to determine whether this inhibition was SPOC specific or whether PP2A-Rts1 was a general MEN inhibitor. To address this question we first examined the importance of MEN activity on SPOC and spindle assembly checkpoint (SAC) activity. We constructed a series of hypermorphic alleles of *TEM1* and tested their behavior in response to challenges to both spindle assembly and spindle positioning. We isolated a hypermorphic allele of *TEM1*, *TEM1-eGFP*. *TEM1-eGFP* suppresses the growth defect of *lte1Δ* cells at 16°C. Other C-terminal tagged alleles of *TEM1* do not display this suppression (Figure 6A). This allele produces about two fold more protein than wild-type *TEM1* (Figure 6B). In addition we examined two overexpression constructs of

TEM1. *TEM1* expressed from a multi copy 2micron plasmid expressed approximately six fold more than wild-type *TEM1* and *TEM1* expressed from the *GAL1-10* promoter produced about 50 fold more protein (Figure 6B). We then tested the ability of these *TEM1* alleles to hyperactivate the MEN and thus bypass the cell cycle arrests caused by the SAC and the SPOC. All three hypermorphic alleles of *TEM1* bypassed the cell cycle arrest caused by spindle position defects to a similar degree (Figure 6C). Cells treated with the spindle poison, nocodazole, activate the SAC which in turn prevents both entry into anaphase and MEN activation in response to microtubule – kinetochore attachment defects (reviewed in (Lew and Burke 2003)). Indeed, deletion of *BUB2* leads to inappropriate activation of the MEN and exit from mitosis in cells treated with nocodazole (Figure 6D; (Fraschini, Formenti et al. 1999)). This is evident from examining the ability of cells to form small buds (termed rebudding) in the presence of nocodazole (Figure 6D;(Hoyt, Totis et al. 1991; Li and Murray 1991; Fraschini, Formenti et al. 1999)). Tem1-eGFP failed to bypass the nocodazole-induced cell cycle arrest (Figure 6D) whereas the intermediate strength allele, 2micron-*TEM1*, displayed an intermediate level of bypass (Figure 6E). The strongest allele, *GAL-TEM1*, displayed the greatest degree of bypass of the nocodazole induced arrest (Figure 7F).

Having established this series of hyperactive *TEM1* alleles, we then compared these alleles to mutants of known SPOC components. Cells lacking *RTS1* or *KIN4* resembled *TEM1-eGFP* cells. The SAC was intact in these cells but the SPOC was not ((D'Aquino, Monje-Casas et al. 2005; Pereira and Schiebel 2005); Figure 6D). In contrast, *bub2*Δ cells most resembled *GAL-TEM1* cells, exhibiting both SAC and SPOC defects (Figure 6F). This finding indicates that like *KIN4*, *RTS1* is not a general inhibitor of the MEN but only exerts its inhibitory function in the SPOC. Additionally, our results suggest that higher levels of MEN activity are required to bypass the SAC than the SPOC.

Discussion

PP2A-Rts1 is a component of the spindle position checkpoint.

Previous studies identified the protein kinase Kin4 as an inhibitor of MEN activity in response to spindle position defects. How the protein kinase was controlled however, was not understood. Based on the correlation between phosphorylation status and presumptive time of *KIN4* function during the cell cycle, we hypothesized that dephosphorylated Kin4 was active and that phosphatases that promoted accumulation of this form would be required for Kin4 function. To test this hypothesis we screened known phosphatases implicated in cell cycle control and identified PP2A and its regulatory subunit Rts1 as being required for Kin4 dephosphorylation. Consistent with the idea that dephosphorylation of Kin4 is indeed required for the protein's function we found that cells lacking PP2A-Rts1 failed to delay exit from mitosis in response to spindle position defects. Our studies also shed light on the mechanism whereby PP2A-Rts1 restrains the MEN when spindles are mis-positioned. The phosphatase does not appear to affect Kin4 kinase activity but instead promotes its association with SPBs, which was previously shown to be essential for SPOC activity (Maekawa, Priest et al. 2007).

Several lines of evidence indicate that PP2A-Rts1 is not a general inhibitor of the MEN but specifically functions in the SPOC by regulating Kin4 localization. Deletion of *RTS1*, like deletion of *KIN4,* leads to a bypass of the spindle position checkpoint arrest but not the nocodazole-induced cell cycle arrest. In contrast, deletion of the MEN inhibitor and target of Kin4, Bub2-Bfa1, leads to a bypass of both checkpoint arrests. The specificity of PP2A-Rts1 towards Kin4 regulation is revealed by the observations that (i) deletion of *KIN4* does not enhance the SPOC defect of the *dyn1Δ rts1Δ* mutant, that (ii) loss of *RTS1* function only alters the phosphorylation state and localization of Kin4 and not other MEN components and that (iii) loss of *RTS1* function suppresses the lethality of overexpression of *KIN4* but not *BFA1*. Attempts to test whether targeting Kin4 to SPBs was the sole function of PP2A-Rts1 in the spindle position checkpoint failed because a *KIN4* allele previously described to constitutively localize to SPBs (*KIN4-SPC72(177-622);* (Maekawa, Priest et al. 2007)*)* is not functional in the checkpoint (Supplemental Figure 3).

PP2A-Rts1 regulation of Kin4 – an additional layer of control in the spindle position checkpoint.

Based on the localization patterns of the MEN activator Lte1 and MEN inhibitor Kin4, we and others previously proposed that bud restricted Lte1 creates a zone of MEN activation in the bud and mother cell restricted Kin4 generates a zone of MEN inhibition in the mother cell ((Bardin, Visintin et al. 2000; Pereira, Hofken et al. 2000; D'Aquino, Monje-Casas et al. 2005); Figure 6G). Because components of the MEN localize to SPBs, movement of the MEN-bearing SPB into the bud would lead to MEN activation and exit from mitosis. In principle, this division of the cell into mitotic exit restrictive and permissive zones would be sufficient to ensure that exit from mitosis only occurs when one SPB and hence half of the nucleus moves into the bud. Our studies described here show that an additional layer of control exists where PP2A-Rts1 controls the association of Kin4 with SPBs that are located in the mother cell. This additional layer of control could provide temporal control over Kin4, restricting access of the kinase to its target to the time when a spindle is present in cells, specifically mitosis. This hypothesis would be consistent with the observed cell cycle regulation of Kin4 phosphorylation.

We do not yet understand how *RTS1* promotes Kin4 loading onto SPBs. PP2A-Rts1 could mobilize Kin4 at the cortex and facilitate its association with SPBs (Figure 6G). Whether the phosphatase does so by dephosphorylating Kin4 or a Kin4 receptor at SPBs is also not known. PP2A-Rts1 not only affects the ability of Kin4 to associate with SPBs in the mother cell but also its association with the mother cell cortex. In wild-type cells Kin4 is restricted to the mother cell cortex during S-phase and early mitosis. In cells lacking *RTS1* less Kin4 is observed at the cortex and localization is not restricted to the mother cell. It is therefore also possible that PP2A-Rts1 plays an important role in the establishment or maintenance of specific Kin4 localization to the mother cell cortex and that perhaps this localization is a prerequisite for Kin4 to load onto SPBs (Figure 6G). Indeed we observe that Kin4 mutants that fail to associate with the mother cell cortex also fail to associate with SPBs during anaphase (L. Y. C. unpublished observations).

A key question raised by the observation that Kin4 phosphorylation changes during the cell cycle is whether PP2A-Rts1 itself is cell cycle and SPOC regulated or whether it is a yet to be identified kinase(s) whose ability to phosphorylate Kin4 is regulated. Despite intense efforts, we have been unsuccessful in identifying kinases that affect phosphorylation and function of Kin4. Regardless of whether the Kin4 kinase(s) is cell cycle regulated, is there evidence that PP2A-Rts1 activity changes during the cell cycle? We do not detect any changes in Rts1 binding to the scaffolding subunit of PP2A, Tpd3, during the cell cycle (Supplemental Figure 4), arguing against cell cycle regulated changes in PP2A subunit composition. There is however evidence that PP2A-Rts1 localization is cell cycle regulated. The protein localizes to centromeric DNA upon cell cycle entry and remains there until anaphase entry. The phosphatase also localizes to the bud neck during late mitosis where it regulates septin dynamics (L. Y. C. unpublished observations,(Gentry and Hallberg 2002; Dobbelaere, Gentry et al. 2003)). Rts1 is not detected on SPBs (L. Y. C. unpublished observations, (Gentry and Hallberg 2002)) arguing against a model where Rts1 association with its targets at the SPB is part of SPOC control. Rather we favor the model where Rts1 is required for localization of Kin4 to the mother cell cortex, which is itself a requirement for SPB localization.

PP2A – a key regulator of chromosome segregation fidelity.

PP2A has previously been implicated in mitotic checkpoint control. The phosphatase together with its targeting subunit Cdc55 is required for cell cycle arrest upon triggering the SAC(Minshull, Straight et al. 1996). Our studies now show that the same phosphatase but with a different targeting subunit is essential for SPOC-induced cell cycle arrest. PP2A however has many other roles in mitotic progression. In controlling chromosome segregation, PP2A-Cdc55 controls the activity of the protein phosphatase Cdc14 during early anaphase as part of the FEAR network and also potentially controls the activity of the APC/C at the metaphase to anaphase transition(Wang and Burke 1997; Queralt, Lehane et al. 2006; Tang and Wang 2006; Yellman and Burke 2006; Chiroli, Rossio et al. 2007). During meiosis, PP2A-Rts1 controls the chromosome segregation factor Sgo1(Riedel, Katis et al. 2006). In all instances where mechanisms are at least partly understood, PP2A control involves the targeted action of the phosphatase at specific

locations in the cell. In the case of the SPOC it is possibly the cell cortex, during meiosis the kinetochore and in the case of the FEAR network the nucleolus. It thus appears that the recurring theme in PP2A control of mitosis is regulation by targeted localization.

Acknowledgements:

We are grateful to James Broach, Steve Elledge, Marco Geymonat, Yu Jiang, Elmar Schiebel and Michael Stark for strains and reagents. We thank Frank Solomon, Fernando Monje-Casas and members of the Amon lab for comments on the manuscript. This work was supported by the National Institutes of Health GM056800 to A.A. and a NSF Pre-doctoral Fellowship to L. Y. C.. A. A is also an investigator of the Howard Hughes Medical Institute.

Materials and Methods:

Yeast Strains and Growth Conditions

All strains are derivatives of W303 (A2587) with the following exceptions: A20126 and A21574 are derivatives of DEY100 (A19130) and A20176 is a derivative of Y398 (A19926). All strains are listed in Supplemental Table 1. Lte1-GFP, Tem1-GFP, Rts1-3HA, *rts1*Δ, Spc42-mCherry and *MET-GFP-KIN4* were constructed by standard PCR based methods(Longtine, McKenzie et al. 1998; Hentges, Van Driessche et al. 2005; Snaith, Samejima et al. 2005). *kin4*^{T209A} was constructed by a two-step gene replacement using the *URA3* gene from *Kluyveromyces lactis*. Growth conditions are described in the figure legends.

Plasmid Construction

The plasmid used to construct the *HIS3MX6:MET-GFP-KIN4* allele, pFA6a-*HIS3MX6:pMET25-GFP* (A1758), was constructed by digesting pFA6a-*HIS3MX6:pGAL-GFP* (Longtine, McKenzie et al. 1998) and a PCR product containing the MET25 promoter with BglII and PacI and ligating the two fragments together.

Immunoblot Analysis

Immunoblot analysis to determine total amount of Kin4-3HA, 3HA-Bfa1, Tem1-3MYC and Lte1-13MYC were performed as described(Bardin, Visintin et al. 2000; Seshan, Bardin et al. 2002; D'Aquino, Monje-Casas et al. 2005). For immunoblot analysis of Kin4-GFP, 3HA-Bub2 and Tem1, cells were incubated for a minimum of 10 minutes in 5% trichloroacetic acid. The acid was washed away with acetone and cells were pulverized with glass beads in 100 μL of lysis buffer (50 mM Tris-Cl pH7.5, 1 mM EDTA, 2.75 mM DTT and complete protease inhibitor cocktail [Roche]) using a bead mill. Sample buffer was added and the cell homogenates were boiled. Kin4-GFP was detected using an anti-GFP antibody (Clontech, JL-8) at 1:1000, 3HA-Bub2 was detected using an anti-HA antibody (Covance, HA.11) at 1:1000 and Tem1 was detected with an anti-Tem1 antibody at 1:1500. Semi-quantitative estimates of relative protein levels of Tem1 were made using ECL Plus (GE Healthcare) and fluorescence imaging. Quantification was performed using NIH Image Quant software. Rts1-3HA was detected using the same anti-HA antibody at 1:1000 and Tpd3 was detected with a rabbit anti-Tpd3 antibody at 1:2000.

Antibody generation

An anti-Tem1 antibody was raised in rabbits against the peptide, CKKLTIPEINEIGDPLLIYKHL. The antibody was then affinity purified using immobilized antigen peptides (Covance).

Fluorescence Microscopy

Indirect in situ immunofluorescence methods and antibody concentrations for Tub1 and Tem1-13MYC were as previously described(Kilmartin and Adams 1984; D'Aquino, Monje-Casas et al. 2005). For simultaneous visualization of nuclei and the mCherry-Tub1 fusion protein, cells were prepared as described (Monje-Casas, Prabhu et al. 2007) with the following modifications: cells were permeabilized with 1% Triton X-100 for 5 minutes and the cells were resuspended in 1 μg/mL Hoechst 3342. For live cell microscopy, cells were grown in YePAD, harvested, resuspended in SC and immediately imaged using a Zeiss Axioplan 2 microscope and a Hamamatsu OCRA-ER digital

camera. Deconvolution was performed with Openlab 4.0.2 software. For quantifications, Z-stacks were taken and the localization was determined.

Spindle position checkpoint assay

Cells were grown to mid-exponential phase and then incubated at 14°C for 24 hours. Cells fixed, stained for the nuclei and spindle and examined for endpoint morphology. Cells that were anucleated, multinucleated or budded with two nuclei in the mother cell body but with a disassembled spindle were counted as bypassed. Budded cells with two nuclei in the mother cell body with an intact anaphase spindle were counted as arrested.

Kin4 Kinase Assays

Kin4 kinase assays were performed as previously (D'Aquino, Monje-Casas et al. 2005)with the following modifications: 30 μL of anti-HA affinity matrix bead slurry (Roche) were used, 3.5 mg of total protein were used per immunoprecipitation, kinase reactions were allowed to run for one hour and the substrate was a mix of 1 μg myelin basic protein and about 5 μg of recombinant MBP-BFA1. MBP-BFA1 was purified as previously described(Geymonat, Spanos et al. 2002). Kinase signal was determined by phosphorimaging and immunoblot signal was determined using ECL Plus (GE Healthcare) and fluorescence imaging. Quantification was performed using NIH Image Quant software.

Co-Immunoprecipitation assays

Approximately 12 OD units of cells were collected, washed once with 10mM Tris-Cl pH7.5 and then lysed with glass beads in a bead mill with lysis buffer (50mM Tris-Cl pH7.5, 150mM NaCl, 1% NP-40, 60mM β-glycerolphosphate, 0.1mM sodium orthovanadate, 15mM para-nitrophenlylphosphate, 1mM DTT and complete protease inhibitor cocktail [Roche]). 1 μg anti-HA antibody (Covance, HA.11) was added to 900 μg of total protein and incubated for 1 hour. 10 μL of pre-swelled protein-G bead slurry (Pierce) were then added to each sample and agitated for 2 hours at 4°C. Beads were then washed six times with wash buffer (50 mM Tris-Cl pH7.5, 150 mM NaCl, 1% NP-40). Sample buffer was added to the beads that were then boiled.

Figure Legends:

Figure 1. PP2A-Rts1 is necessary for Kin4 dephosphorylation

(A) Wild-type cells expressing a Kin4-3HA fusion (A11779) were arrested in G1 with 5 μg/mL α factor and released into pheromone free media. After 70 minutes, 10 μg/mL α factor was added to prevent entry into a subsequent cell cycle. Cell cycle stage was determined by spindle and bud morphology. Kin4-3HA was monitored by western blot. An asterisk indicates a cross-reacting band with the HA antibody.

(B) Wild-type (A11779), *cdc14-3* (A19111), *glc7-12* (A19808), *sit4-102* (A20176), *pph3Δ pph21Δ pph22-12* (A20126), *cdc55Δ* (A19804) and *rts1Δ* (A20187) cells expressing a Kin4-3HA fusion were grow to exponential phase at room temperature and then shifted to 37°C (t=0). Samples were taken at the indicated times to examine Kin4-3HA mobility. Vph1 was used as a loading control.

(C) Quantification of (B). The phosphorylation ratio is the intensity of the slower migrating band divided by the intensity of the faster migrating band.

Figure 2. PP2A-Rts1 functions in the spindle position checkpoint

(A) A *dyn1Δ rts1Δ* mutant (A21725) carrying a mCherry-Tub1 marker (red) was grown at 14°C for 24 hours. The DNA was visualized by Hoechst staining (blue). Cells with the arrested morphology are budded and have two DNA masses spanned by an anaphase spindle in the mother cell. Cells with the bypassed morphology have no DNA masses or multiple DNA masses but with disassembled spindles or spindles indicative of cell cycle progression after improper mitotic exit.

(B) Wild-type (A2587), *dyn1*Δ (A17349), *dyn1*Δ *kin4*Δ (A17351), *dyn1*Δ *rts1*Δ (20310), *rts1*Δ (A20312), *dyn1*Δ *cdc55*Δ (A21520), *cdc55*Δ (A15396), *dyn1*Δ

*pph3*Δ *pph21Δ pph22-12* (A21574), *pph3Δ pph21Δ pph22-12* (A19130) and *dyn1*Δ *rts1*Δ *kin4*Δ (A21538) were grown as described in (A). Cells were stained for tubulin by indirect immuno-fluorescence and the DNA was stained with DAPI. $n \geq 100$ cells per sample. Gray bars represent the percentage of cells with the arrested morphology and white bars represent the percentage of cells with the bypassed morphology. Error bars represent SEM.

Figure 3. PP2A-Rts1 affects Kin4 phosphorylation but not other MEN components

(A) *GAL-GFP-KIN4* (A11997), *GAL-GFP-KIN4 rts1*Δ (A20893), *GAL-GFP-BFA1* (A3487), *GAL-GFP-BFA1 rts1*Δ (A20892), *rts1*Δ (A20312), *GAL-GFP-KIN4 bub2Δ* (A18792) and *bub2Δ* (A1863) cells were spotted on plates containing either dextrose or galactose and raffinose. The first spot represents growth of approximately $3x10^4$ cells and each subsequent spot is a 10 fold serial dilution.

(B-F) Wild-type and *rts1*Δ cells expressing (B) Kin4-3HA (A11779 and A20187), (C) 3HA-Bfa1 (A4378 and A21540), (D) 3HA-Bub2 (A21921 and A22064), (E) Tem1-3MYC (A1828 and A21539) or (F) Lte1-13MYC (A22669 and A22669) were analyzed as described in Figure 1A. Vph1, Pgk1 and a cross reacting band with the HA antibody (labeled with an asterisk) were used as loading controls.

Figure 4. Localization of Kin4 to the mother SPB during anaphase requires *RTS1*

(A-C) Wild-type (A19900) and *rts1*Δ (A20918) cells expressing Kin4-GFP and mCherry-Tub1 fusion proteins were treated as described in Figure 1A. Samples were taken every 15 minutes for 2 hours after release and the cells were imaged live. Serial sections spanning the entire cell were collected to ensure imaging of all spindle poles. Panels in (A) show deconvolved images from 20 serial sections. Kin4-GFP is in green and mCherry-Tub1 is in red. Levels of Kin4-GFP for equal ODs of culture are shown in (B). Pgk1 was used

as a loading control. Quantification of Kin4-GFP colocalization with spindle poles is shown in (C). $n \geq 100$ for interphase, metaphase and anaphase cells. $n \geq 40$ for the rarer telophase cells. Error bars represent SEM.

Figure 5. SPOC induced Kin4 localization to spindle poles requires *RTS1*

(A-C) Wild-type (A19902) and *rts1*Δ (A21732) cells expressing Kin4-GFP and SPC42-mCherry fusion proteins were treated with 1.5 μg/mL nocodazole for 90 minutes. Cells were analyzed as described in Figure 5A. Kin4-GFP is in green and Spc42-mCherry is in red. Quantification of Kin4-GFP colocalization with the SPC42-mCherry marker is shown in (B). $n \geq 50$ for each strain. Error bars represent SEM. Levels of Kin4-GFP for equal ODs of culture are shown in (C). Pgk1 was used as a loading control.

(D-E) *dyn1*Δ (A21720) and *dyn1*Δ *rts1*Δ (A22878) cells expressing Kin4-GFP and mCherry-Tub1 proteins were grown to exponential phase and then shifted to 14°C for 24 hours. Cells were collected and analyzed as described in Figure 5A. Quantification of Kin4-GFP colocalization with spindle poles is shown in (E). $n \geq 50$. Error bars represent SEM.

(F) Wild-type (A2587) and *MET-GFP-KIN4* (A23232) were spotted on SC medium supplemented with 8 mM methonine or SC medium lacking methonine and incubated at 30°C for 24 hours. The first spot represents growth of approximately $3x10^4$ cells and each subsequent spot is a 10 fold serial dilution. This overexpression allele was used instead of *GAL-GFP-KIN4* for single cell analysis of the effects of *KIN4* overexpression due to the low viability of *rts1Δ* mutants when grown in raffinose.

(G) *MET-GFP-KIN4* (A23358) and *MET-GFP-KIN4 rts1*Δ (A23357) cells expressing a mCherry-Tub1 fusion protein were grown and arrested with α factor inYePAD + 8 mM methonine. After 2.5 hours of arrest, cells were washed and resuspended in SC –MET + α factor media and the arrest was held for an additional 30 minutes. Cells were then released into pheromone free SC –

MET media. Anaphase cells were counted for co-localization of GFP-Kin4 with the ends of the spindle. n $\geq$ 100. Error bars represent SEM.

(H-I) *dyn1*Δ and *dyn1*Δ *rts1*Δ cells expressing mCherry-Tub1 and (F) Bfa1-eGFP (A21723 and A21722) or (G) Bub2-eGFP (A21724 and A21725) were analyzed as described in (D) and (E). n $\geq$ 50. Error bars represent SEM.

(J) *dyn1*Δ (A12123), *dyn1*Δ *kin4*Δ (A12122) and *dyn1*Δ *rts1*Δ (A22636) cells expressing a Tem1-13MYC fusion protein were grown as described in (D) and stained for tubulin and Tem1-13MYC by indirect immuno-fluorescence. n $\geq$ 50. Error bars represent SEM.

Figure 7. The SPOC and SAC are bypassed by differing levels of MEN activation

(A) Wild-type (A2587), *lte1Δ* (A18591), *lte1Δ TEM1-eGFP* (A21483), *lte1Δ TEM1-GFP* (A22567) and *lte1Δ TEM1-3MYC* (A4365) cells were spotted on YePAD plates and incubated at 30°C and 16°C. Pictures shown represent growth from 2 days for the 30°C condition and 4 days for 16°C. The first spot represents growth of approximately $3x10^4$ cells and each subsequent spot is a 10 fold serial dilution.

(B) Whole cell lysates from 0.13 ODs of cells were analyzed by western blot for Tem1 levels in the wild-type (A2587), *TEM1-eGFP* (A21089), Yep13-*TEM1* (A23122) and *GAL-TEM1* (A2441) strains. A23122 was grown in SC-LEU for plasmid maintenance and A2441 was pregrown in YePA + 2% raffinose and induced with addition of 2% galactose for 2 hours.

(C) *dyn1*Δ (A17349), *dyn1*Δ *TEM1-eGFP* (A22811), *dyn1*Δ YEp13 (A23125), *dyn1*Δ YEp13-*TEM1* (A19104) and *dyn1*Δ *GAL-TEM1* (A23117) were grown and analyzed as described in Figures 2A and 2B with the following modifications: strains carrying YEp13 plasmids were pregrown in SC-LEU and then transferred to YePAD medium prior to temperature shift and strains A17349 and A23117 for the experiment in the third panel were pregrown in YePA + 2% raffinose and the GAL promoter was induced two hours prior to temperature shift with the addition of 2% galactose. n $\geq$ 100 and error bars represent SEM.

(D) Wild-type (A2587), *mad1Δ* (A928), *bub2Δ* (A1863), *kin4*Δ (A17865), *rts1Δ* (A20312) and *TEM1-eGFP* (A21089) cells were grown and arrested in G1 as described in Figure 1A and subsequently released into media containing 1.5 μg/mL nocodazole. Additional 0.75 ug/mL nocodazole was added at 220 minutes after release to maintain the metaphase block. Samples were taken every 20 minutes for microscopic analysis. $n \geq 100$.

(E) YEp13 (A23121), Yep13-*TEM1* (A23122) and YEp13 *bub2Δ* (A23120) cells were grown and analyzed as in 1A and 7D with the following modification: strains were pregrown in SC-LEU to maintain the plasmid and then transferred to YePAD medium prior to pheromone arrest.

(F) Wild-type (A2587), *GAL-TEM1* (A2441) and *bub2Δ* (A1863) cells were grown and analyzed as in 1A and 7D with the following modifications: strains were grown and arrested in YePA + 2% raffinose and the GAL promoter was induced half an hour prior to release with the addition of 2% galactose.

(G) Model for the role of *RTS1* in the control of *KIN4*. See discussion for further details.

Supplemental Figure 1. Loss of *RTS1* function does not affect the kinase activity of Kin4

(A) *dyn1*Δ (A17349), *dyn1Δ kin4Δ* (A17351) and *dyn1*Δ *kin4*^{T209A}Δ (A22736) cells were grown for 24 hours at 14°C. The DNA was visualized by DAPI staining and microtubules were stained by indirect immuno-fluorescence. Gray bars represent the percentage of cells with the arrested morphology and white bars represent the percentage of cells with the bypassed morphology.

(B) Wild-type cells expressing either a Kin4-3HA or a kin4^{T209A}-3HA (kinase dead) fusion (A11779 or A22119) and *rts1*Δ cells expressing either a Kin4-3HA or a kin4^{T209A}-3HA fusion (A20187 or A22120) were grown to exponential phase and arrested with 1.5 μg/mL nocodazole for 2 hours. Kin4 associated kinase activity (top, Kin4 kinase), immunoprecipitated Kin4-3HA (second row, IPed Kin4), total amount of Kin4-3HA in extracts (third row, input Kin4) and levels of Bfa1 substrate (as monitored by Coomassie stain) added to the kinase reaction

(bottom, Bfa1) is shown. The band that is shown for Kin4 associated kinase activity and total Bfa1 substrate is the first major degradation product of MBP-Bfa1 as described in Maekawa et al., 2007 and was the dominant signal. An asterisk indicates a cross reacting band with the HA antibody.

(C) Normalized activity of (B) was calculated as kinase activity divided by immunoprecipitated Kin4. Relative activity was calculated as normalized activity of the sample divided by the normalized activity of the wild-type sample.

Supplemental Figure 2. Tem1 and its regulators display normal localization in the *rts1*Δ mutant

(A-C) Wild-type and *rts1*Δ cells expressing mCherry-Tub1 and (A) Bfa1-eGFP (A21608 and A21729), (B) Bub2-eGFP (A21610 and A21730) or (C) Tem1-GFP (A22556 and A22667) were analyzed as described in Figures 4A and 4C.

(D) Wild-type (A22632) and *rts1*Δ (A22631) cells expressing Lte1-GFP and mCherry-Tub1 were analyzed as described in Figure 4A. Panels display typical cells and all localization trends were completely penetrant in all cells examined.

Supplemental Figure 3. *KIN4-SPC72(177-622)* is a loss of function allele of *KIN4*

(A) *dyn1*Δ (A17349), *dyn1Δ kin4Δ* (A17351) *dyn1Δ rts1Δ* (A20310) *dyn1Δ rts1Δ KIN4-SPC72(177-622)* (A22062) and *dyn1*Δ *KIN4-SPC72(177-622)* (A22063) cells were grown for 24 hours at 14°C. The DNA was visualized by DAPI staining and microtubules were stained by indirect immuno-fluorescence. Gray bars represent the percentage of cells with the arrested morphology and white bars represent the percentage of cells with the bypassed morphology.

Supplemental Figure 4. Rts1 and Tpd3 are associated throughout the cell cycle

(A-B) Wild-type cells expressing an Rts1-3HA (A20757) fusion protein were grown as described in Figure 1A. Rts1-3HA was immunoprecipitated using an HA antibody and the ability to co-immunoprecipitate Tpd3 was examined by western blot with an antibody against Tpd3. Cell cycle progression was monitored by spindle morphology (B).

Supplemental Table 1: Strain List

Strain	Relevant genotype	Source
928	*MATa mad1Δ::URA3*	
1828	*MATa TEM1-3MYC*	
1863	*MATa bub2Δ::HIS3MX6*	
2441	*MATa ura3:GAL-TEM1:URA3*	
2587	*MATa ade2-1 leu2-3 ura3 trp1-1 his3-11,15 can1-100 GAL+ psi+*	
3487	*MATa HIS3MX6:GAL-GFP-BFA1*	
4365	*MATa lte1Δ::KanMX6 TEM1-3MYC*	
4378	*MATa 3HA-BFA1*	
11779	*MATa KIN4-3HA:KanMX6*	
11997	*MATa HIS3MX6:GAL-GFP-KIN4*	
12122	*MATa dyn1Δ::URA3 TEM1-13MYC:HIS3MX6 3HA-CDC14 kin4Δ::KanMX6*	
12123	*MATa dyn1Δ::URA3 TEM1-13MYC:HIS3MX6 3HA-CDC14*	
15396	*MATa cdc55Δ::KanMx6*	
17349	*MATa dyn1Δ::URA3*	
17351	*MATa kin4Δ::KanMX6 dyn1Δ::URA3*	
17865	*MATa kin4Δ::KanMX6*	
18591	*MATa lte1Δ::KanMX6*	
18792	*MATa HIS3MX6:GAL-GFP-KIN4 bub2Δ::HIS3MX6*	
19104	*MATa dyn1Δ::URA3 Yep13-TEM1*	
19111	*MATa KIN4-3HA:KanMX6 cdc14-3*	
19130	*MATa pph21Δ1::HIS3 pph22-12 pph3Δ1::LYS2 ssd1-d2*	DEY100[1]
19804	*MATa KIN4-3HA:TRP1 cdc55Δ::KanMX6*	
19808	*MATa trp1-1:glc7-12:TRP1 glc7Δ::LEU2 KIN4-3HA:KanMX6*	

19900	*MATa ura3:mCherry-TUB1:URA3 KIN4-GFP:HIS3MX6*	
19902	*MATa SPC42-mCherry:NatMX6 KIN4-GFP:HIS3MX6*	
19926	*MATa sit4Δ::HIS3 ssd1-d1 Ycp50-sit4-102 (URA/CEN)*	Y398[2]
20126	*MATa pph21Δ1::HIS3 pph22-12 pph3Δ1::LYS2 ssd1-d2 KIN4-3HA:KanMX6*	
20176	*MATa sit4Δ::HIS3 ssd1-d1 KIN4-3HA:KanMX6 Ycp50-sit4-102 (URA/CEN)*	
20187	*MATa KIN4-3HA::KanMX6 rts1Δ::NatMX6*	
20310	*MATa rts1Δ::NatMX6 dyn1Δ::URA3*	
20312	*MATa rts1Δ::NatMX6*	
20757	*MATa RTS1-3HA:KanMX6*	
20892	*MATa HIS3MX6:GAL-GFP-BFA1 rts1Δ::NatMX6*	
20893	*MATa HIS3MX6:GAL-GFP-KIN4 rts1Δ::NatMX6*	
20918	*MATa ura3:mCherry-TUB1:URA3 KIN4-GFP:HIS3MX6 rts1Δ::NatMX6*	
21089	*MATa TEM1-yEGFP:HIS3MX6*	
21483	*MATa lte1Δ::KanMX6 TEM1-yEGFP:HIS3MX6*	
21520	*MATa cdc55Δ::KanMX6 dyn1Δ::URA3*	
21538	*MATa rts1Δ::NatMX6 kin4Δ::TRP1 dyn1Δ::URA3*	
21539	*MATa TEM1-3 rts1Δ::NatMX6*	
21540	*MATa rts1Δ::NatMX6 3HA-BFA1*	
21574	*MATa pph21Δ1::HIS3 pph22-12 pph3Δ1::LYS ssd1-d2 dyn1Δ::NatMX6*	
21608	*MATa ura3:mCherry-TUB1:URA3 BFA1-yEGFP:KanMX6*	
21610	*MATa ura3:mCherry-TUB1:URA3 BUB2-yEGFP:KanMX6*	
21720	*MATa ura3:mCherry-TUB1:URA3 KIN4-GFP:HIS3MX6 dyn1Δ::URA3*	
21722	*MATa ura3:mCherry-TUB1:URA3 BFA1-yEGFP:KanMX6 dyn1Δ::URA3 rts1Δ::NatMX6*	
21723	*MATa ura3:mCherry-TUB1:URA3 BFA1-yEGFP:KanMX6 dyn1Δ::URA3*	

21724	*MATa ura3:mCherry-TUB1:URA3 BUB2-yEGFP:KanMX6 dyn1Δ::URA3*	
21725	*MATa ura3:mCherry-TUB1:URA3 BUB2-yEGFP:KanMX6 dyn1Δ::URA3 rts1Δ::NatMX6*	
21729	*MATa ura3:mCherry-TUB1:URA3 BFA1-yEGFP:KanMX6 rts1Δ::NatMX6*	
21730	*MATa ura3:mCherry-TUB1:URA3 BUB2-yEGFP:KanMX6 rts1Δ::NatMX6*	
21732	*MATa SPC42-mCherry:NatMX6 KIN4-GFP:HIS3MX6 rts1Δ::NatMX6*	
21921	*MATa 3HA-BUB2*	yFH649-2[3]
22062	*MATa dyn1Δ::URA3 rts1Δ::NatMx6 LEU2:KIN4 -SPC72(177-622):kin4Δ::KL-URA3:Kin4'3'UTR:KanMX6*	
22063	*MATa dyn1Δ::URA3 LEU2:KIN4-SPC72(177-622): kin4Δ::KL-URA3:Kin4'3'UTR:KanMX6*	
22064	*MATa 3HA-BUB2 rts1Δ::NatMX6*	
22119	*MATa Kin4T209A-3HA:KanMX6*	
22120	*MATa Kin4T209A-3HA:KanMX6 rts1Δ::NatMX6*	
22556	*MATa ura3:mCherry-TUB1:URA3 TEM1-GFP:HIS3MX6*	
22567	*MATa lte1Δ::NatMX6 TEM1-GFP:HIS3MX6*	
22631	*MATa ura3:mCherry-TUB1:URA3 LTE1-GFP:KanMX6 rts1Δ::NatMX6*	
22632	*MATa ura3:mCherry-TUB1:URA3 LTE1-GFP:KanMX6*	
22636	*MATa dyn1Δ::URA3 TEM1-13MYC:HIS3MX6 rts1Δ::NatMX6*	
22667	*MATa ura3:mCherry-TUB1:URA3 TEM1-GFP:HIS3MX6 rts1Δ::NatMX6*	
22668	*MATa LTE1-13MYC:KanMX6*	
22669	*MATa LTE1-13MYC:KanMX6 rts1Δ::NatMX6*	
22736	*MATa KIN4T209A:Kin4-3'UTR:KanMX6 dyn1Δ::URA3*	
22811	*MATa dyn1Δ::URA3 TEM1-yEGFP:HIS3MX6*	

22878 *MATa ura3:mCherry-TUB1:URA3 KIN4-GFP:HIS3MX6 dyn1Δ::HIS3MX6 rts1Δ::NatMX6*

23117 *MATa dyn1Δ::URA3 ura3:GAL-TEM1:URA3*

23120 *MATa Yep13 bub2Δ::HIS3MX6*

23121 *MATa Yep13*

23122 *MATa Yep13-TEM1*

23125 *MATa dyn1*Δ::URA3 Yep13

23232 *MATa HIS3MX6:MET-GFP-KIN4*

23357 *MATa HIS3MX6:MET-GFP-KIN4 ura3:mCherry-TUB1:URA3 rts1Δ::NatMX6*

23358 *MATa HIS3MX6:MET-GFP-KIN4 ura3:mCherry-TUB1:URA3*

References:

[1] Evans, D. R. and M. J. Stark (1997). "Mutations in the Saccharomyces cerevisiae type 2A protein phosphatase catalytic subunit reveal roles in cell wall integrity, actin cytoskeleton organization and mitosis." Genetics **145**(2): 227-41.

[2] Wang, H., X. Wang, et al. (2003). "Interaction with Tap42 is required for the essential function of Sit4 and type 2A phosphatases." Mol Biol Cell **14**(11): 4342-51.

[3] Hu, F. and S. J. Elledge (2002). "Bub2 is a cell cycle regulated phospho-protein controlled by multiple checkpoints." Cell Cycle **1**(5):351-355.

Bardin, A. J., R. Visintin, et al. (2000). "A mechanism for coupling exit from mitosis to partitioning of the nucleus." Cell **102**(1): 21-31.
Bloecher, A., G. M. Venturi, et al. (2000). "Anaphase spindle position is monitored by the BUB2 checkpoint." Nat Cell Biol **2**(8): 556-8.
Cheng, J., N. Turkel, et al. (2008). "Centrosome misorientation reduces stem cell division during ageing." Nature **456**(7222): 599-604.
Chiroli, E., V. Rossio, et al. (2007). "The budding yeast PP2ACdc55 protein phosphatase prevents the onset of anaphase in response to morphogenetic defects." J Cell Biol **177**(4): 599-611.
D'Aquino, K. E., F. Monje-Casas, et al. (2005). "The protein kinase Kin4 inhibits exit from mitosis in response to spindle position defects." Mol Cell **19**(2): 223-34.
Dobbelaere, J., M. S. Gentry, et al. (2003). "Phosphorylation-dependent regulation of septin dynamics during the cell cycle." Dev Cell **4**(3): 345-57.
Evans, D. R. and M. J. Stark (1997). "Mutations in the Saccharomyces cerevisiae type 2A protein phosphatase catalytic subunit reveal roles in cell wall integrity, actin cytoskeleton organization and mitosis." Genetics **145**(2): 227-41.
Fesquet, D., P. J. Fitzpatrick, et al. (1999). "A Bub2p-dependent spindle checkpoint pathway regulates the Dbf2p kinase in budding yeast." Embo J **18**(9): 2424-34.
Fraschini, R., E. Formenti, et al. (1999). "Budding yeast Bub2 is localized at spindle pole bodies and activates the mitotic checkpoint via a different pathway from Mad2." J Cell Biol **145**(5): 979-91.
Gentry, M. S. and R. L. Hallberg (2002). "Localization of Saccharomyces cerevisiae protein phosphatase 2A subunits throughout mitotic cell cycle." Mol Biol Cell **13**(10): 3477-92.
Geymonat, M., A. Spanos, et al. (2002). "Control of mitotic exit in budding yeast. In vitro regulation of Tem1 GTPase by Bub2 and Bfa1." J Biol Chem **277**(32): 28439-45.
Geymonat, M., A. Spanos, et al. (2003). "In vitro regulation of budding yeast Bfa1/Bub2 GAP activity by Cdc5." J Biol Chem **278**(17): 14591-4.
Hentges, P., B. Van Driessche, et al. (2005). "Three novel antibiotic marker cassettes for gene disruption and marker switching in Schizosaccharomyces pombe." Yeast **22**(13): 1013-9.
Hoyt, M. A., L. Totis, et al. (1991). "S. cerevisiae genes required for cell cycle arrest in response to loss of microtubule function." Cell **66**(3): 507-17.
Hu, F., Y. Wang, et al. (2001). "Regulation of the Bub2/Bfa1 GAP complex by Cdc5 and cell cycle checkpoints." Cell **107**(5): 655-65.
Jaspersen, S. L., J. F. Charles, et al. (1999). "Inhibitory phosphorylation of the APC regulator Hct1 is controlled by the kinase Cdc28 and the phosphatase Cdc14." Curr Biol **9**(5): 227-36.
Jiang, Y. (2006). "Regulation of the cell cycle by protein phosphatase 2A in Saccharomyces cerevisiae." Microbiol Mol Biol Rev **70**(2): 440-9.
Kilmartin, J. V. and A. E. Adams (1984). "Structural rearrangements of tubulin and actin during the cell cycle of the yeast Saccharomyces." J Cell Biol **98**(3): 922-33.
Lee, J., H. S. Hwang, et al. (1999). "Ibd1p, a possible spindle pole body associated protein, regulates nuclear division and bud separation in Saccharomyces cerevisiae." Biochim Biophys Acta **1449**(3): 239-53.

Lee, S. E., L. M. Frenz, et al. (2001). "Order of function of the budding-yeast mitotic exit-network proteins Tem1, Cdc15, Mob1, Dbf2, and Cdc5." Curr Biol **11**(10): 784-8.
Lew, D. J. and D. J. Burke (2003). "The spindle assembly and spindle position checkpoints." Annu Rev Genet **37**: 251-82.
Li, R. (1999). "Bifurcation of the mitotic checkpoint pathway in budding yeast." Proc Natl Acad Sci U S A **96**(9): 4989-94.
Li, R. and A. W. Murray (1991). "Feedback control of mitosis in budding yeast." Cell **66**(3): 519-31.
Li, Y. Y., E. Yeh, et al. (1993). "Disruption of mitotic spindle orientation in a yeast dynein mutant." Proc Natl Acad Sci U S A **90**(21): 10096-100.
Longtine, M. S., A. McKenzie, 3rd, et al. (1998). "Additional modules for versatile and economical PCR-based gene deletion and modification in Saccharomyces cerevisiae." Yeast **14**(10): 953-61.
Luca, F. C., M. Mody, et al. (2001). "Saccharomyces cerevisiae Mob1p is required for cytokinesis and mitotic exit." Mol Cell Biol **21**(20): 6972-83.
Maekawa, H., C. Priest, et al. (2007). "The yeast centrosome translates the positional information of the anaphase spindle into a cell cycle signal." J Cell Biol **179**(3): 423-36.
Mah, A. S., J. Jang, et al. (2001). "Protein kinase Cdc15 activates the Dbf2-Mob1 kinase complex." Proc Natl Acad Sci U S A **98**(13): 7325-30.
Minshull, J., A. Straight, et al. (1996). "Protein phosphatase 2A regulates MPF activity and sister chromatid cohesion in budding yeast." Curr Biol **6**(12): 1609-20.
Monje-Casas, F., V. R. Prabhu, et al. (2007). "Kinetochore orientation during meiosis is controlled by Aurora B and the monopolin complex." Cell **128**(3): 477-90.
O'Connell, C. B. and Y. L. Wang (2000). "Mammalian spindle orientation and position respond to changes in cell shape in a dynein-dependent fashion." Mol Biol Cell **11**(5): 1765-74.
Pereira, G., T. Hofken, et al. (2000). "The Bub2p spindle checkpoint links nuclear migration with mitotic exit." Mol Cell **6**(1): 1-10.
Pereira, G. and E. Schiebel (2005). "Kin4 kinase delays mitotic exit in response to spindle alignment defects." Mol Cell **19**(2): 209-21.
Queralt, E., C. Lehane, et al. (2006). "Downregulation of PP2A(Cdc55) phosphatase by separase initiates mitotic exit in budding yeast." Cell **125**(4): 719-32.
Riedel, C. G., V. L. Katis, et al. (2006). "Protein phosphatase 2A protects centromeric sister chromatid cohesion during meiosis I." Nature **441**(7089): 53-61.
Seshan, A., A. J. Bardin, et al. (2002). "Control of Lte1 localization by cell polarity determinants and Cdc14." Curr Biol **12**(24): 2098-110.
Shirayama, M., Y. Matsui, et al. (1994). "Isolation of a CDC25 family gene, MSI2/LTE1, as a multicopy suppressor of ira1." Yeast **10**(4): 451-61.
Shirayama, M., Y. Matsui, et al. (1994). "The yeast TEM1 gene, which encodes a GTP-binding protein, is involved in termination of M phase." Mol Cell Biol **14**(11): 7476-82.
Shou, W., J. H. Seol, et al. (1999). "Exit from mitosis is triggered by Tem1-dependent release of the protein phosphatase Cdc14 from nucleolar RENT complex." Cell **97**(2): 233-44.

Snaith, H. A., I. Samejima, et al. (2005). "Multistep and multimode cortical anchoring of tea1p at cell tips in fission yeast." Embo J **24**(21): 3690-9.
Tang, X. and Y. Wang (2006). "Pds1/Esp1-dependent and -independent sister chromatid separation in mutants defective for protein phosphatase 2A." Proc Natl Acad Sci U S A **103**(44): 16290-5.
Visintin, R., K. Craig, et al. (1998). "The phosphatase Cdc14 triggers mitotic exit by reversal of Cdk-dependent phosphorylation." Mol Cell **2**(6): 709-18.
Visintin, R., E. S. Hwang, et al. (1999). "Cfi1 prevents premature exit from mitosis by anchoring Cdc14 phosphatase in the nucleolus." Nature **398**(6730): 818-23.
Wang, H., X. Wang, et al. (2003). "Interaction with Tap42 is required for the essential function of Sit4 and type 2A phosphatases." Mol Biol Cell **14**(11): 4342-51.
Wang, Y. and D. J. Burke (1997). "Cdc55p, the B-type regulatory subunit of protein phosphatase 2A, has multiple functions in mitosis and is required for the kinetochore/spindle checkpoint in Saccharomyces cerevisiae." Mol Cell Biol **17**(2): 620-6.
Yeh, E., R. V. Skibbens, et al. (1995). "Spindle dynamics and cell cycle regulation of dynein in the budding yeast, Saccharomyces cerevisiae." J Cell Biol **130**(3): 687-700.
Yellman, C. M. and D. J. Burke (2006). "The role of Cdc55 in the spindle checkpoint is through regulation of mitotic exit in Saccharomyces cerevisiae." Mol Biol Cell **17**(2): 658-66.
Zachariae, W., M. Schwab, et al. (1998). "Control of cyclin ubiquitination by CDK-regulated binding of Hct1 to the anaphase promoting complex." Science **282**(5394): 1721-4.

A

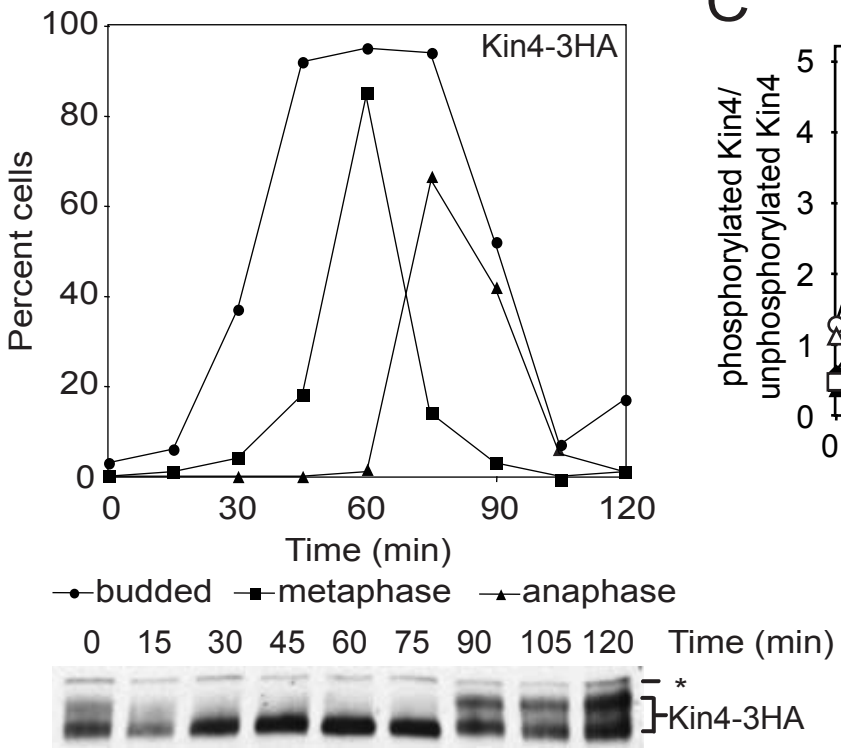
Kin4-3HA
Percent cells
100
80
60
40
20
0
0
30
60
90
120
Time (min)
budded
metaphase
anaphase

0 15 30 45 60 75 90 105 120 Time (min)
*
Kin4-3HA

C

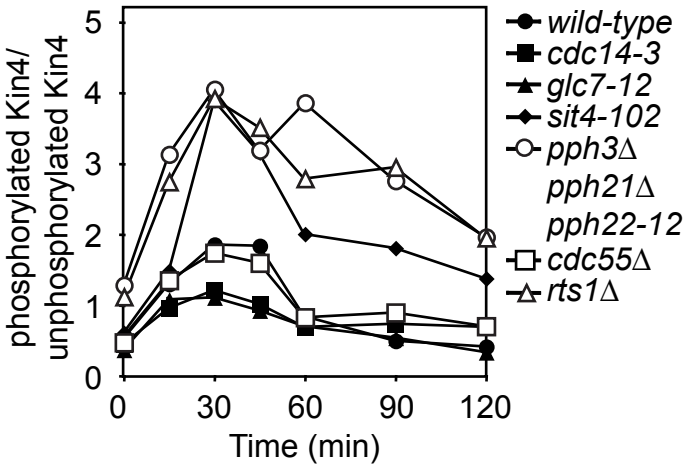
phosphorylated Kin4/
unphosphorylated Kin4
5
4
3
2
1
0
0
30
60
90
120
Time (min)
wild-type
cdc14-3
glc7-12
sit4-102
pph3Δ
pph21Δ
pph22-12
cdc55Δ
rts1Δ

B

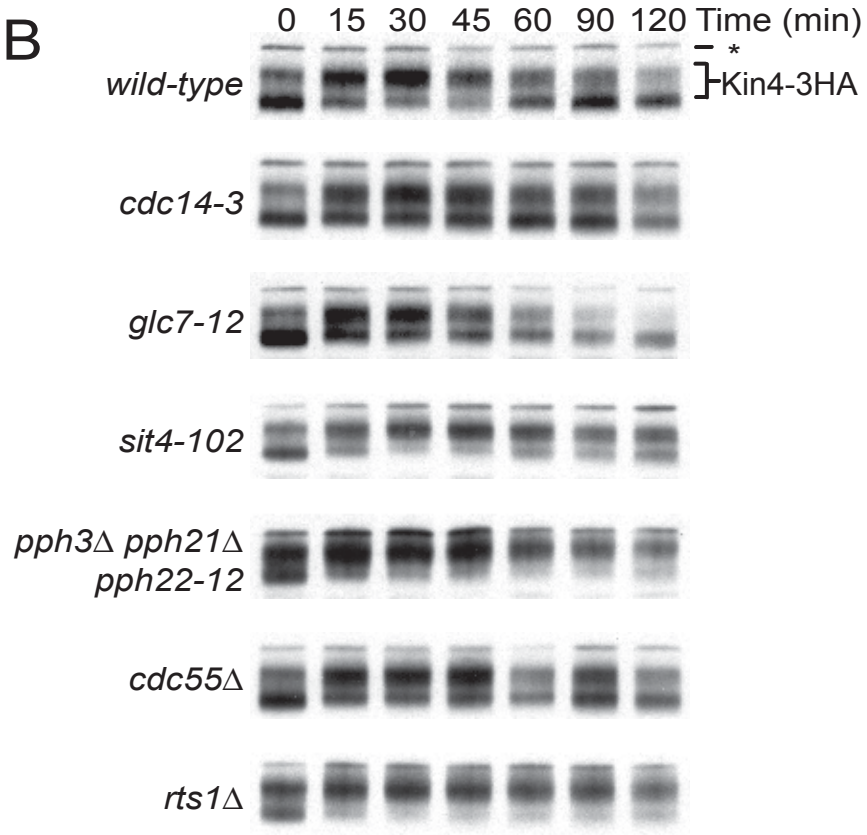
0 15 30 45 60 90 120 Time (min)
*
Kin4-3HA
wild-type
cdc14-3
glc7-12
sit4-102
pph3Δ pph21Δ
pph22-12
cdc55Δ
rts1Δ

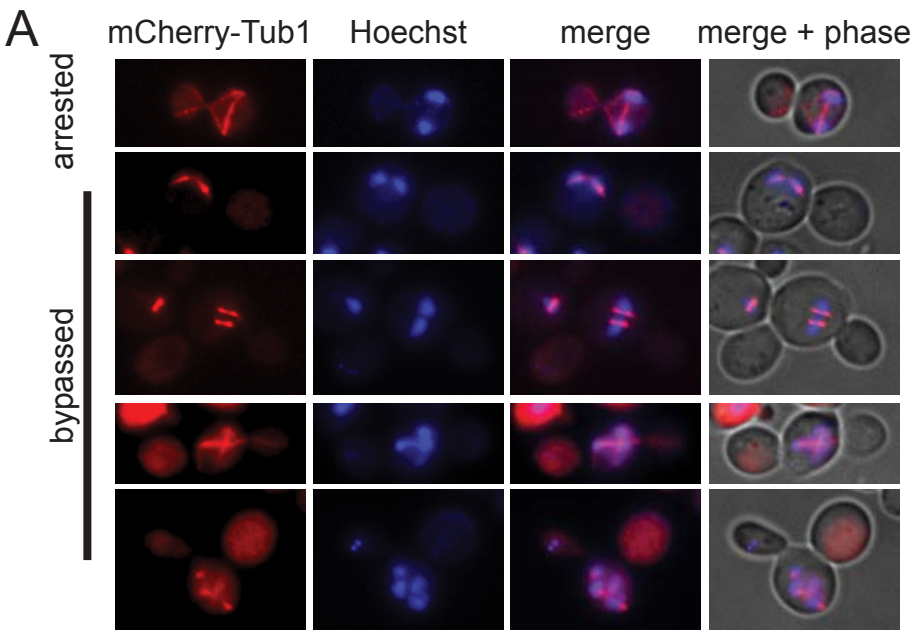
A
mCherry-Tub1
Hoechst
merge
merge + phase
arrested
bypassed

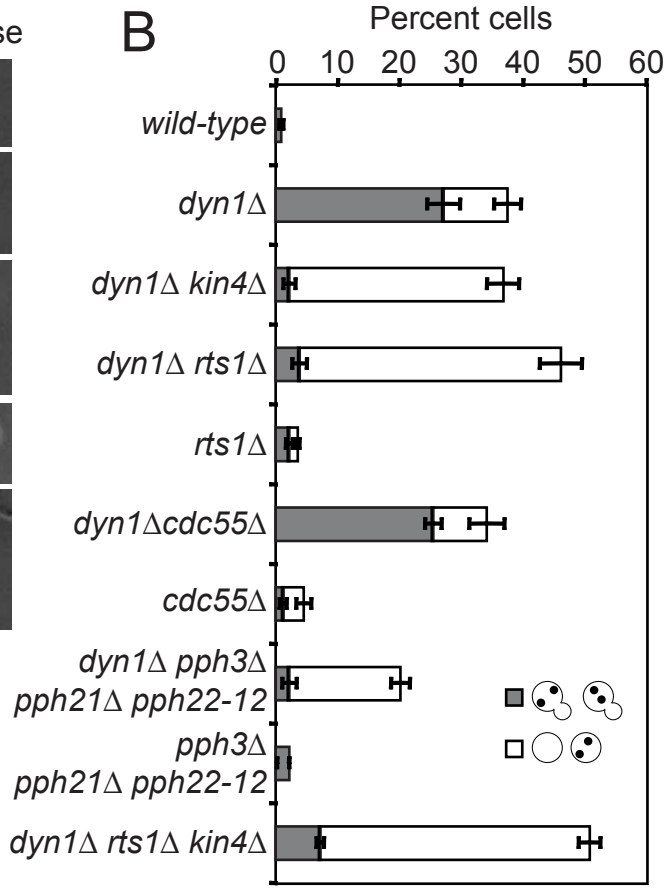
B
Percent cells
0
10
20
30
40
50
60
wild-type
dyn1Δ
dyn1Δ kin4Δ
dyn1Δ rts1Δ
rts1Δ
dyn1Δcdc55Δ
cdc55Δ
dyn1Δ pph3Δ pph21Δ pph22-12
pph3Δ pph21Δ pph22-12
dyn1Δ rts1Δ kin4Δ

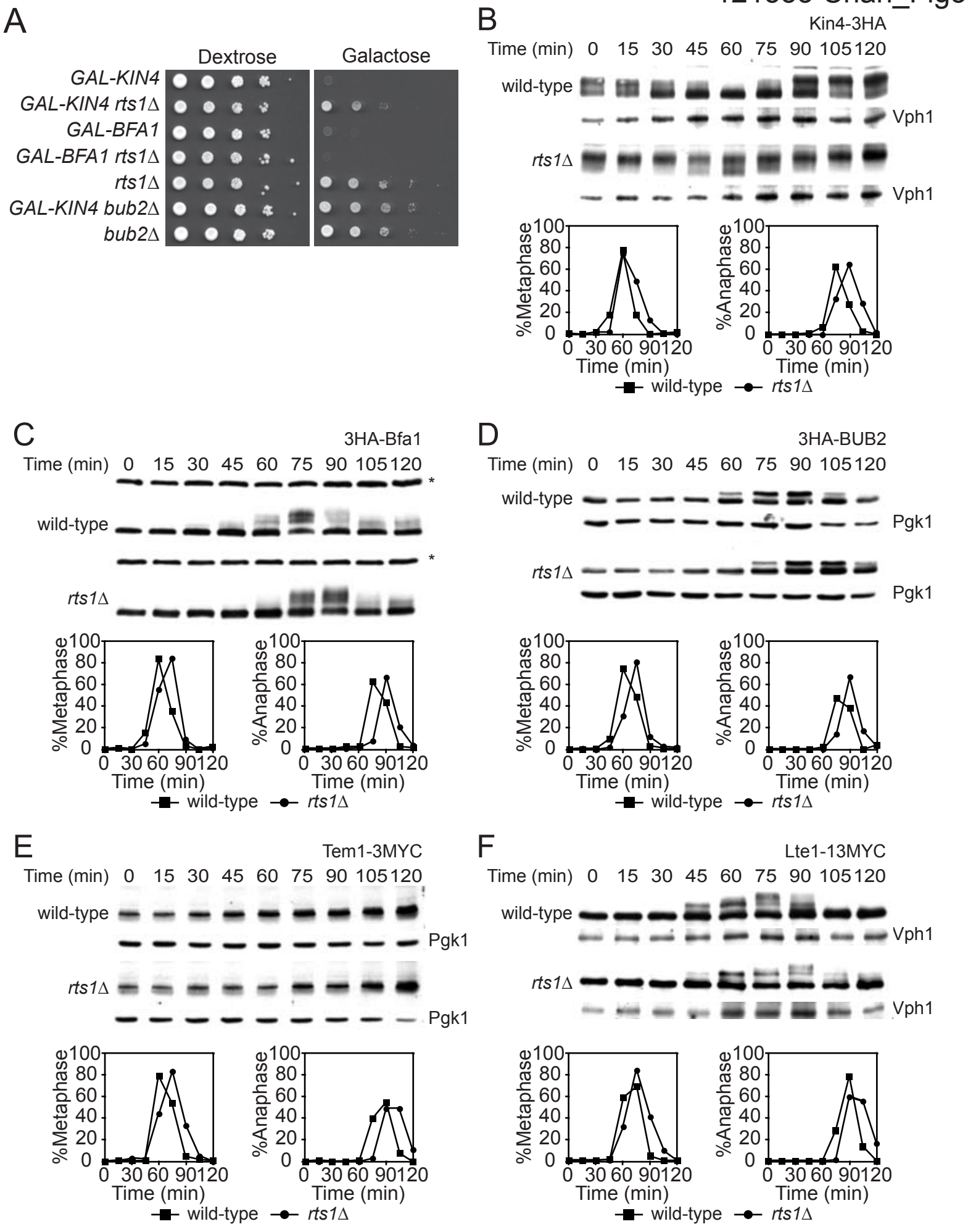
A
Dextrose
Galactose
GAL-KIN4
GAL-KIN4 rts1Δ
GAL-BFA1
GAL-BFA1 rts1Δ
rts1Δ
GAL-KIN4 bub2Δ
bub2Δ
B
Kin4-3HA
Time (min) 0 15 30 45 60 75 90 105 120
wild-type
Vph1
rts1Δ
Vph1
%Metaphase
%Anaphase
0 30 60 90 120
Time (min)
wild-type
rts1Δ
C
3HA-Bfa1
Time (min) 0 15 30 45 60 75 90 105 120
wild-type
*
*
rts1Δ
%Metaphase
%Anaphase
0 30 60 90 120
Time (min)
wild-type
rts1Δ
D
3HA-BUB2
Time (min) 0 15 30 45 60 75 90 105 120
wild-type
Pgk1
rts1Δ
Pgk1
%Metaphase
%Anaphase
0 30 60 90 120
Time (min)
wild-type
rts1Δ
E
Tem1-3MYC
Time (min) 0 15 30 45 60 75 90 105 120
wild-type
Pgk1
rts1Δ
Pgk1
%Metaphase
%Anaphase
0 30 60 90 120
Time (min)
wild-type
rts1Δ
F
Lte1-13MYC
Time (min) 0 15 30 45 60 75 90 105 120
wild-type
Vph1
rts1Δ
Vph1
%Metaphase
%Anaphase
0 30 60 90 120
Time (min)
wild-type
rts1Δ

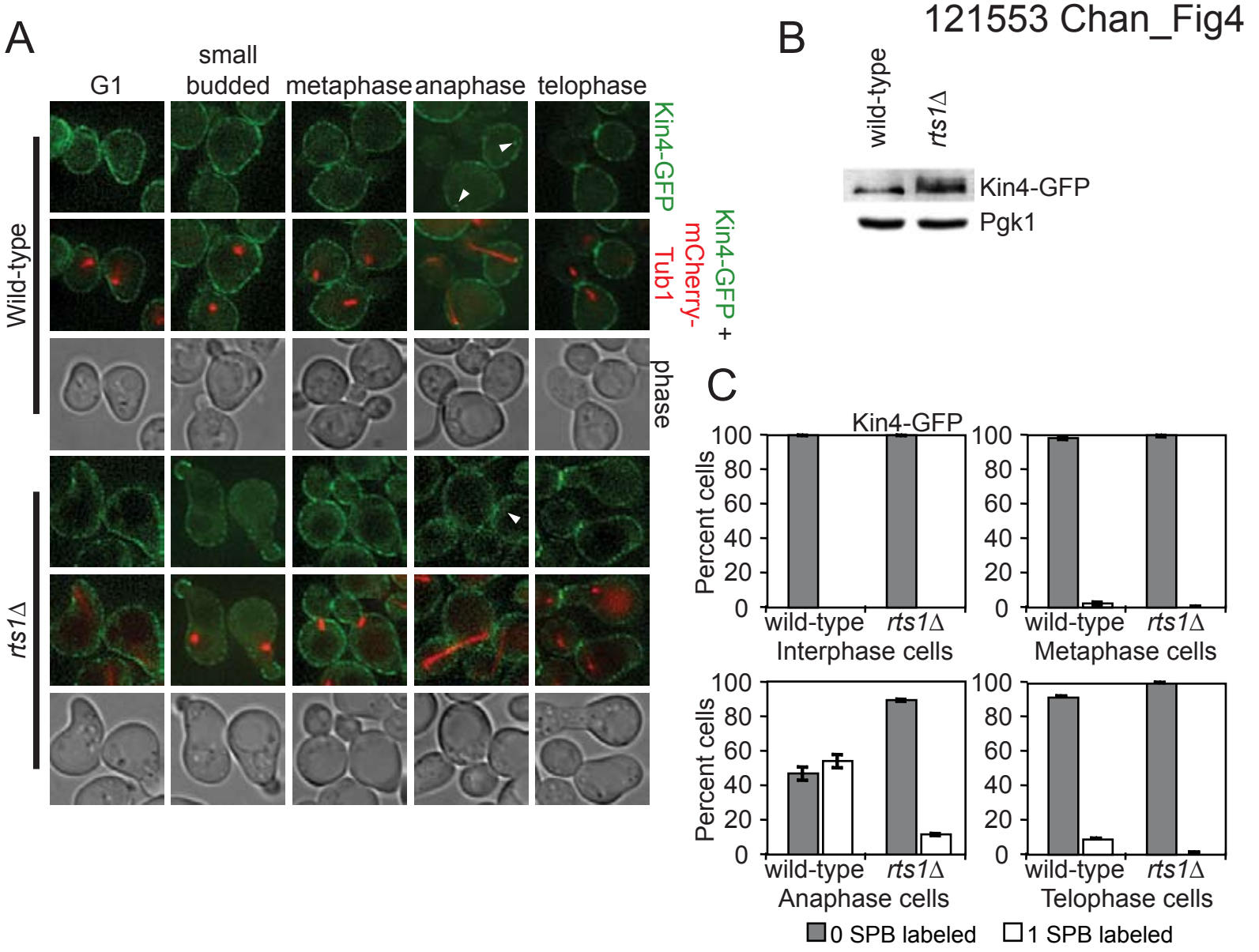
A
G1
small budded
metaphase
anaphase
telophase
Wild-type
rts1Δ
Kin4-GFP
Kin4-GFP + mCherry-Tub1
phase
B
wild-type
rts1Δ
Kin4-GFP
Pgk1
C
Kin4-GFP
Percent cells
100
80
60
40
20
0
wild-type
rts1Δ
Interphase cells
Metaphase cells
Anaphase cells
Telophase cells
0 SPB labeled
1 SPB labeled

121553 Chan_Fig5

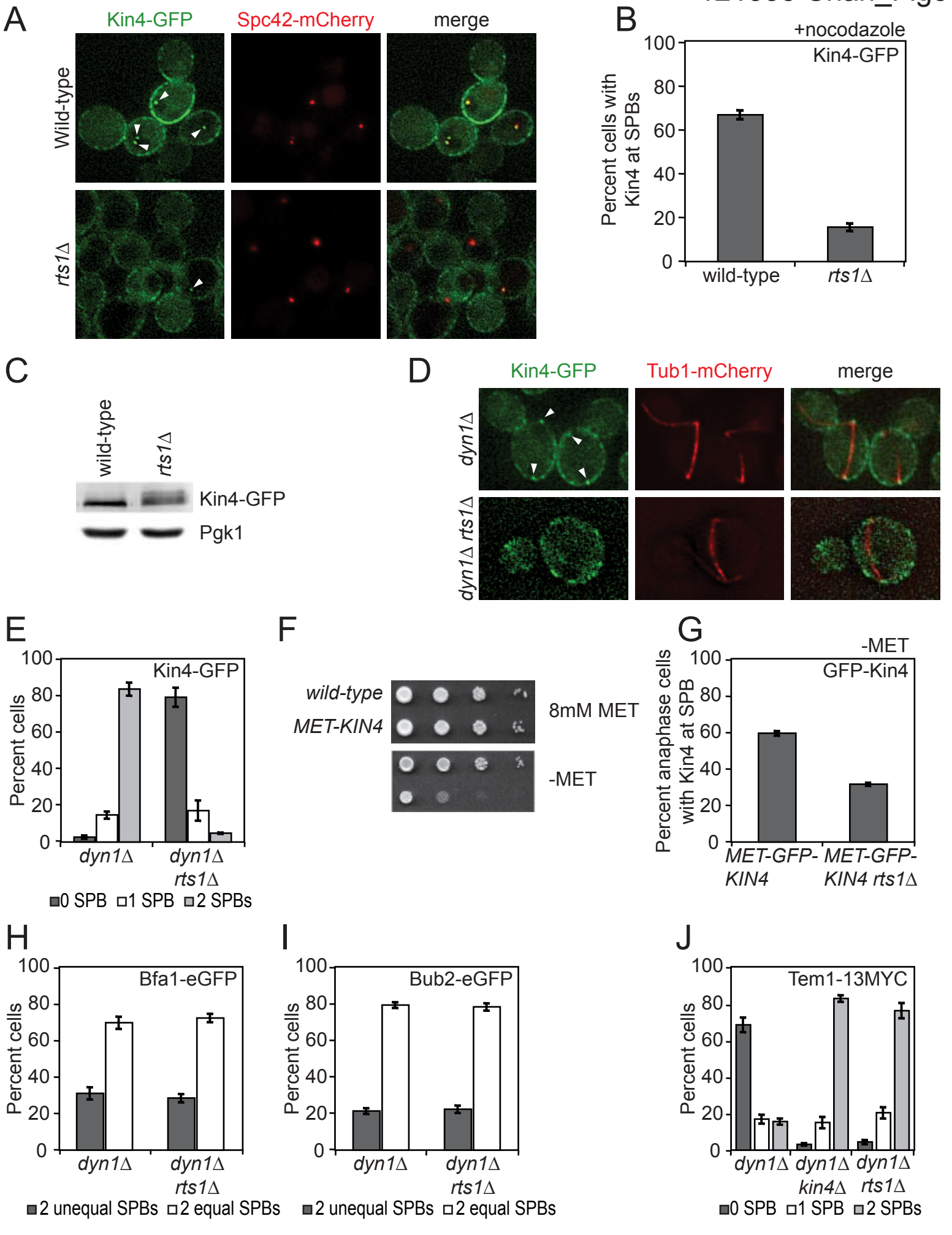

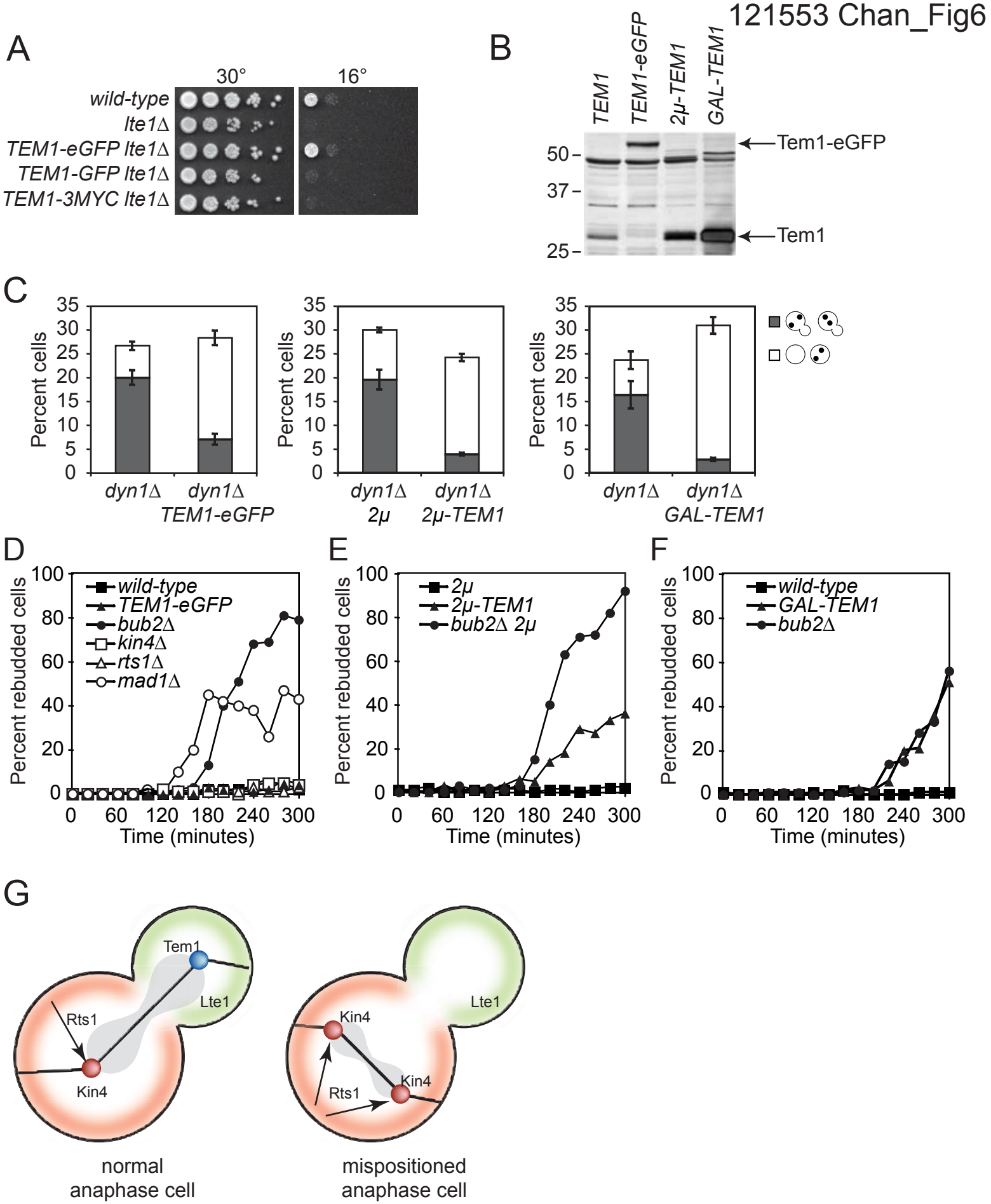
A
30°
16°
wild-type
lte1Δ
TEM1-eGFP lte1Δ
TEM1-GFP lte1Δ
TEM1-3MYC lte1Δ
B
TEM1
TEM1-eGFP
2μ-TEM1
GAL-TEM1
50
37
25
Tem1-eGFP
Tem1
C
Percent cells
dyn1Δ
dyn1Δ TEM1-eGFP
dyn1Δ 2μ
dyn1Δ 2μ-TEM1
dyn1Δ GAL-TEM1
D
Percent rebudded cells
wild-type
TEM1-eGFP
bub2Δ
kin4Δ
rts1Δ
mad1Δ
Time (minutes)
E
2μ
2μ-TEM1
bub2Δ 2μ
F
wild-type
GAL-TEM1
bub2Δ
G
Tem1
Lte1
Rts1
Kin4
normal anaphase cell
mispositioned anaphase cell